Structure and dynamics of protonated Mg$_2$SiO$_4$: An ab-initio molecular dynamics study

MICHAEL HAIBER, PIETRO BALLONE, AND MICHELE PARRINELLO

Max-Planck-Institut für Festkörperforschung, Heisenbergstrasse 1, 70569 Stuttgart, Germany

ABSTRACT

We studied structural and dynamical properties of H$^+$ absorbed in Mg$_2$SiO$_4$ by ab-initio molecular dynamics. We first calculated the $T = 0$ equation of state of pure forsterite as a function of pressure, and we determined the relative stabilities of the olivine, β-spinel, and spinel polymorphs. The results show that the ab-initio model successfully reproduces the known structural properties of the system. In the protonated phases, in agreement with experimental evidence, our computations show that H$^+$ is absorbed preferentially in the β-spinel phase. The most stable absorption site is located close to the O1 atom, which is coordinated by five Mg^{2+} cations and not directly bound to Si. In addition to this stable absorption site, the computation reveals other low-energy positions, forming an extended network of hydrogen bonds, that could play an important role in the diffusion of H$^+$ in β-spinel. We analyze the dependence of structure and dynamics of the pure and protonated phases as a function of temperature and pressure.

INTRODUCTION

Widely accepted models of the Earth assume that Mg$_2$SiO$_4$-based minerals are the major component of the upper mantle, which extends to a depth of 660 km. Olivine [(Mg$_{1-x}$Fe$_x$)$_2$SiO$_4$, $x \approx 0.1$] is the most common and possibly the most studied member of this family of minerals, which includes many other compounds and displays a surprising variety of chemical and physical properties. This variability, mainly because of the Mg$_2$SiO$_4$ component (forsterite), is at the origin of several important phenomena of geophysical interest. The well-known discontinuity in seismic waves velocities at a depth of 410 km marks the transformation of Mg$_2$SiO$_4$ from the olivine (α phase) to the spinel structure (γ phase), with a narrow but important intermediate region of stability for the β-spinel polymorph (Ringwood 1970). A second major discontinuity at a depth of 660 km is associated to the disproportionation of forsterite into MgSiO$_3$ perovskite and MgO (Ringwood 1975).

Recent experimental (Bell 1992; Young 1993; Inoue 1994) and theoretical (Smyth 1987, 1994) studies have shown that H may dissolve in Mg$_2$SiO$_4$ with strong preferential binding in the β phase. The saturation concentration is 3 wt% H$_2$O at the conditions estimated for the mantle β phase, although the actual value is expected to be significantly smaller, i.e., in the range of ~200 ppm (Wood 1995). Even at this low concentration, a massive amount of H$_2$O could reside in the mantle at depths below 410 km in the form of protonated β-Mg$_2$SiO$_4$, and this could affect several features of this important region, including the size and structure of the transition boundary between the α and β phases and the melting line of the latter. Global properties, such as the mantle electrical con-

ductivity, could also be affected significantly (Hirsch 1990: Karato 1990).

Determining the phase diagram of this complex system at a quantitative level and understanding the behavior of its many components test the ingenuity of geophysicists and geochemists alike, especially because most of the key phenomena occur under conditions difficult to reproduce in the laboratory.

It is generally felt that computational methods could play a crucial role in assessing the properties of these minerals at the atomistic level, especially where ab-initio modeling is used to describe the chemical interactions and simulation algorithms are introduced to account for temperature effects. These last requirements are fully met by the density-functional-based ab-initio simulation method of Car and Parrinello (Car 1985; Jones 1989) that achieves quantitative accuracy in the description of structural and dynamical properties of complex systems. Progress in both the method and computer performance now allows extensive and reliable simulations of minerals at the conditions prevailing in the Earth's interior (Wentzcovitch et al. 1993, 1995; Lin 1994; McConnell 1995).

Our study concentrates on forsterite and its ability to dissolve H under various conditions of pressure and temperature. We first test our ab-initio model by computing the $T = 0$ equation of state of pure Mg$_2$SiO$_4$ as a function of pressure, and we determine the stability range of its olivine, β-spinel, and spinel polymorphs. The results are in remarkable agreement with the available experimental data. Then we determine the lowest energy absorption site for a proton in olivine and β-spinel by a combination of structural relaxation and molecular dynamics. We consider both Mg$_2$SiO$_4$ samples with one additional H$^+$, whose charge is compensated by a homogeneous back-

ground, and neutral samples with two protons and one Mg^{2+} vacancy. In this last case, we study the interaction of the defects by comparing the energy for different relative positions of the protons and the vacancy.

Simulations for pure Mg$_2$SiO$_4$ at high temperature were also performed (as described in the Appendix) and provided a benchmark for characterizing the thermal properties of the protonated phase.

THE AB-INITIO MODEL

Our model is based on the density functional theory (Hohenberg 1964), according to which the electronic ground-state energy E_0 for a given configuration ($\mathbf{R}_I$) of the atomic nuclei is the minimum of a unique functional E of the electron density $\rho(r)$:

$$E_0[(\mathbf{R}_I)] = \,^{\min}_\rho E[\rho \,|\, (\mathbf{R}_I)]. \tag{1}$$

An explicit evaluation of E is obtained by expressing $\rho(r)$ as the sum of independent electron orbitals [$\psi_{\mathbf{k}}^i(r)$]:

$$\rho(r) = \int_{\mathrm{BZ}} d\mathbf{k} \sum_i f_{\mathbf{k}}^i |\Psi_{\mathbf{k}}^i(r)|^2. \tag{2}$$

The integration is over the Brillouin zone of the crystal, and $f_{\mathbf{k}}^i$ are occupation numbers. The functional $E[\rho]$ is given by Kohn (1965):

$$E[\rho]$$

$$= \sum_i \int_{\mathrm{BZ}} d\mathbf{k} f_{\mathbf{k}}^i \left\langle \Psi_{\mathbf{k}}^i \left| -\frac{1}{2}\Delta \right| \Psi_{\mathbf{k}}^i \right\rangle + \frac{1}{2} \int\int \frac{\rho(r)\rho(r')}{|r - r'|} \, dr \, dr'$$

$$+ \sum_i \int_{\mathrm{BZ}} d\mathbf{k} f_{\mathbf{k}}^i \left\langle \Psi_{\mathbf{k}}^i | \hat{V}^{e-I}[(\mathbf{R}_I)] | \Psi_{\mathbf{k}}^i \right\rangle + E_{\mathrm{XC}}[\rho] + E_{i-i} \tag{3}$$

where the first term is a kinetic energy contribution, the second term is the classical Hartree energy of the electron density ρ, $\hat{V}^{e-I}$ is the potential on the electrons because of the nuclei, E_{XC} is the so-called exchange-correlation energy, and E_{i-i} is the classical Coulomb energy of the nuclei. In the local density approximation, which is used in our computation, E_{XC} is given by:

$$E_{\mathrm{XC}} = \int \rho(r)\epsilon[\rho(r)]dr \tag{4}$$

where $\epsilon_{\mathrm{XC}}[\rho]$ is the XC energy density (per electron) of the uniform electron gas at density ρ. The minimization is performed by expanding ($\psi_{\mathbf{k}}^i$) in a basis set and optimizing E with respect to the expansion coefficient. In our computation the orbitals are expanded in a basis of plane waves:

$$\Psi_{\mathbf{k}}^i = \sum_G c_{\mathbf{G},\mathbf{k}}^i \exp[i(\mathbf{k} + \mathbf{G})r] \tag{5}$$

where $\mathbf{G}$ are reciprocal lattice vectors, and the sum includes all the plane waves up to a kinetic energy cut off, E_c, to be specified below. The optimization is performed either by direct minimization of the functional E with

respect to $c_{\mathbf{G},\mathbf{k}}^i$ or by self-consistent, iterative diagonalization of the equivalent Euler-Lagrange equations:

$$\left\{ -\frac{1}{2}\Delta + \int \frac{\rho(r')}{|r - r'|} \, dr + \hat{V}^{e-I} + \epsilon[\rho(r)] \right.$$

$$\left. + \rho(r)\frac{\partial}{\partial\rho(r)}\epsilon[\rho(r)] \right\} \Psi_{\mathbf{k}}^i = \Lambda_{\mathbf{k}}^i \Psi_{\mathbf{k}}^i. \tag{6}$$

The terms $\Lambda_{\mathbf{k}}^i$, the so-called Kohn-Sham (KS) eigenvalues, are Lagrange multipliers introduced to ensure the ortho-normality of the orbitals.

As an additional approximation, we only treat explicitly the valence electrons, and we replace nuclei and core electrons by an ab-initio, norm-conserving non-local pseudopotential (Pickett 1989). For Mg and Si we used the pseudopotentials produced and tested by Stumpf et al. (1990). For H and O we used two different pseudopotentials: (1) Benchmark computations performed by Stumpf et al. (1990) pseudopotentials, and (2) for most of the actual computations we used soft Troullier-Martins type of pseudopotentials (Troullier 1991), whose transferability has been tested against the Stumpf et al. results. The non-locality of the pseudopotentials is expressed by means of the Kleinman-Bylander construction (Kleinman 1982; Pickett 1989).

The wave functions determined by minimizing the functional $E[\rho]$ for a fixed ionic configuration were used to compute the Hellmann-Feynmann forces on the ions:

$$\mathbf{F}_I = -\frac{\partial E[\rho]}{\partial \mathbf{R}_I} = -\sum_i \int_{\mathrm{BZ}} d\mathbf{k} f_{\mathbf{k}}^i \left\langle \Psi_{\mathbf{k}}^i \left| \frac{\partial \hat{V}^{e-i}[(\mathbf{R}_I)]}{\partial \mathbf{R}_I} \right| \Psi_{\mathbf{k}}^i \right\rangle \tag{7}$$

In turn, these allow us to optimize the structures by quasi-static relaxation or to generate molecular dynamics (MD) trajectories as described by Galli (1991). During MD runs, the orbitals (ψ^i) are propagated in time by the adiabatic dynamics of Car and Parrinello (1985), also described by Galli (1991). Appendix 1 reports additional information on the parameters used in our computations.

THE $T = 0$ K EQUATION OF STATE OF PURE Mg$_2$SiO$_4$

To test the reliability of the ab-initio model and to select the parameters for the MD simulation described below, we studied the $T = 0$ equation of state for pure Mg$_2$SiO$_4$ as a function of pressure, and we determined the relative stability of the olivine, β-spinel, and spinel polymorphs by comparing their enthalpies.

Throughout our paper we use the conventions of Megaw (1973), Baur (1971), and Wyckoff (1968) to name the inequivalent atoms in the three Mg$_2$SiO$_4$ phases. These structures are all based on the close packing of O anions and are identified by the stacking of the compact planes (hcp for α, fcc for β and γ), the distortion of the O atom lattice, and the distribution of the cations among the tetrahedral and octahedral interstitial sites. Both olivine and spinel are orthosilicates, characterized by well-defined SiO$_4$ tetrahedra, whereas β-spinel, a sorosilicate, has the Si$_2$O$_7$ unit (two tetrahedra joined at one vertex,
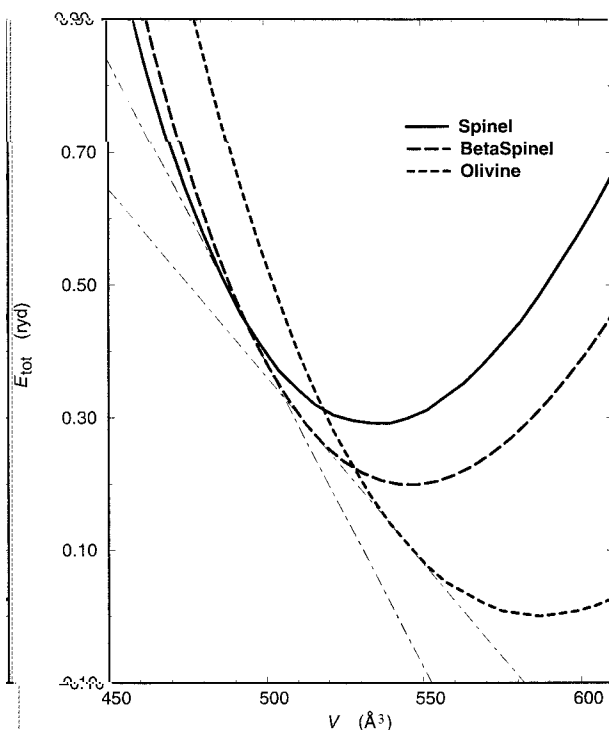
FIGURE 1. Total energy E_{tot} vs. volume V for olivine, β-spinel, and spinel structures. The curves are the Murnaghan interpolation to the computed DFT-LDA total energies. Each curve has been fitted to at least seven points. The straight lines are the common tangent to the olivine, β-spinel, and spinel curves.

with two edges almost colinear) as a building block. In all these structures, for each tetrahedral site that is occupied by the Si^{4+} cations, there are seven others that are empty and, as we describe below, play an important role in accommodating the stresses generated when pressure is applied. The Mg^{2+} cations occupy one-half of the available octahedral sites.

TABLE 1. Parameters of the Murnaghan equation of state at $T = 0$

	α	β	γ
V_0 (Å³)	586.6 (580.0)	545.2 (537.6)	533.5 (526.5)
a (Å)	10.20 (10.21)	8.29 (8.248)	8.11 (8.075)
b (Å)	6.02 (5.98)	11.50 (11.444)	
c (Å)	9.56 (9.50)	5.72 (5.696)	
B_0 (Mbar)	1.37	1.79	1.89
B_0'	3.75	4.26	4.08
C (eV)	0.00	2.69	3.95

Note: The theoretical values for the three phases olivine (α), β-spinel (β), and spinel (γ) were obtained by a least-squares fit of the computed $E(V)$ data. The experimental values, reported in parentheses, are from Megaw (1973) and Baur (1971) for olivine and β-spinel and Sung (1987) for spinel. For all the structures V_0 and C refer to a conventional cell of 56 atoms.

For each structure we started from the atomic positions given by Sung (1987) and Baur (1971). Only a few of the coordinates were not determined by symmetry and were carefully optimized: Self-consistent forces were computed and the structure was relaxed until the residual energy gradient on each atom was <0.1 eV/Å. The b/a and c/a ratios for olivine and β-spinel were also optimized by imposing the condition that, for each volume, the applied pressure is hydrostatic. The maximum anisotropy in the stress that was acceptable at the end of the optimization was 2%. The optimized lattice parameters and atomic positions as a function of pressure are shown in Tables 4, 5, and 6.[1]

The total energy vs. volume for the three structures is reported in Figure 1, with the corresponding interpolations by the Murnaghan equation of state (Yin 1982):

$$E(V) = \frac{B_0 V}{B_0'}\left[\frac{(V_0/V)^{B_0'}}{B_0' - 1} + 1\right] + C \qquad (8)$$

whose parameters are listed in Table 1. The comparison with the available experimental data, also reported in Table 1, is satisfactory.

The double-tangent construction applied to the $E(V)$ curves of Figure 1 predicts that olivine is stable up to 12.4 GPa, beyond which it transforms to β-spinel. The relative volume change associated with this first transformation is 5.6%. With further increasing pressure, the system undergoes a second structural transformation from the β to the γ phase, at 20.0 GPa, with a relative volume change of 1.8%. According to the diagrams published by Akimoto (1977), and attributed to Kawada (1977), the β-spinel phase of pure Mg₂SiO₄ is stable from 12 to 17 GPa at 1073 K, from 12 to 19 GPa at 1273 K, and from 14 to 21 GPa at 1473 K. This phase diagram was revised by Morishima (1994). A comparison with the phase diagram published in recent papers (e.g., Rubie 1994; Akaogi 1989) shows that the uncertainty in the phase boundaries are on the order of 2 GPa. Extrapolation of these data to low temperature suggests that the α → β transition occurs at 10 GPa, and the β → γ occurs at 15 GPa, in fair agreement with our results. The total volume change from olivine to spinel (i.e., including the stability range of β-spinel) is 10.5%, in good agreement with the experiments. The computed enthalpy changes are 6.6 kcal/mol for the α → β transformation and 3.2 kcal/mol for the β → γ transformation, again in good agreement with the experimental data [7.6 ± 0.7 kcal/mol, and 1.6 ± 0.9 kcal/mol, respectively (Akaogi 1984)].

The olivine and β-spinel phases, which have non-trivial b/a and c/a ratios, display a clear tendency toward a more cubic structure (i.e., b/a and c/a tend toward one) with increasing pressure. As could be expected, the different

---

[1] For a copy of Tables 4, 5, 6, and 7, order Document AM-97-648 from the Business Office, Mineralogical Society of America, 1015 Eighteenth Street, Suite 601, Washington, DC 20036, U.S.A. Please remit $5.00 in advance. Deposit items may also be available on the American Mineralogist web site, refer to the inside back cover of a current issue for web address.

TABLE 2. Ionic charges computed by Mulliken population analysis

	Mg	Mg1	Mg2	Mg3	O	O1	O2	O3	O4	Si	Unas-signed charge
Olivine		1.72	1.72			−1.21	−1.22	−1.21		1.91	4.03
β-spinel		1.65	1.69	1.64		−1.43	−1.06	−1.21	−1.22	2.08	4.08
Spinel	1.66				−1.21					1.99	3.80

Notes: Charges were computed at the equilibrium volume of each structure with a minimal atomic basis. The unassigned charge corresponds to a conventional cell of 56 atoms and 256 electrons.

structural units (i.e., filled and empty tetrahedra and octahedra) react in different ways to applied pressure, whereas the behavior of each is very similar in the three phases of Mg$_2$SiO$_4$. The SiO$_4^{4+}$ tetrahedra (including those fused into Si$_2$O$_7$ units) represent the stiffest component in each phase. Their rigidity is compensated by the large change of volume of the empty tetrahedra. The compressibility of the octahedral sites does not show great variations between empty and Mg^{2+} filled ones and is similar to the overall compressibility. Our results for the relative compressibilities of the different structural units are in agreement with experimental data (Hazen 1976) and consistent with the vibrational analysis of Mg$_2$SiO$_4$ by Hofmeister (1987) and Chopelas (1991), which assumes that the SiO$_4^{4+}$ tetrahedra are the least deformable units in the system. They are also qualitatively similar to the experimental data for the closely related Ni$_2$SiO$_4$ system (Finger 1979).

The charge distribution in the system has been analyzed in terms of the Mulliken population (Szabo 1989), computed by projecting the Kohn-Sham eigen-states (expressed in terms of plane waves) on a minimal basis of atomic orbitals. Also note that this analysis is more qualitative than quantitative, with results sensitive to the atomic basis. The Mulliken charges are reported in Table 2. As expected, olivine and spinel have very similar ionic character. In contrast, β-spinel displays intriguing differences, which are the basis for the discussion of protonation in the next section: Mg, Si, and the majority of the O atoms again have ionic charges similar to those of the other two structures. However, two of the O atoms have significantly different ionic charges: (1) O1 atom, which is not directly bonded to Si, but is coordinated by five Mg cations arranged in a square pyramid geometry and (2) the O2 atom, which bridges the two (deformed) tetrahedra forming the Si$_2$O$_7$ unit. As first pointed out by Smyth (1987, 1994), O1 is underbonded, and in our computation this is reflected in an electron charge excess of 0.2 e with respect to the "normal" O atoms (as estimated from the Mulliken population analysis, see Table 2). This charge is not drawn evenly from all the other atoms in the system but is pulled only from O2, which displays an anomalously low ionic charge.

Ab-initio MD has been used to perform finite-temperature simulations for pure Mg$_2$SiO$_4$ (spanning ~1 ps), whose results are briefly discussed in Appendix 2.

H IN Mg$_2$SiO$_4$: STATIC PROPERTIES

As mentioned in the introduction, experiments have shown that nominally anhydrous Mg$_2$SiO$_4$ may actually contain a significant amount of H, the absorption being energetically more favorable in the β-spinel phase. In the experimental samples, the excess positive charge carried by H$^+$ is compensated by Mg^{2+} vacancies. Because the concentration of H$^+$ is likely to be in the range of ~200 ppm, the Mg^{2+} vacancies and the H$^+$ impurities are not expected to be bound, because, at the temperatures of geophysical interest, entropy always prevails over the energy cost of breaking the pairs. As a consequence, the equilibrium position of H$^+$ and their dynamics are not directly influenced by the Mg^{2+} vacancies, which act like a homogeneous background of negative charge, ensuring global system neutrality. We simulated this situation by performing computations for Mg$_2$SiO$_4$ samples of 56 atoms in the olivine. β-spinel, or spinel structures plus one proton. The excess charge is compensated by a uniform negative charge distribution. For each phase, the computation was performed at a volume close to the minimum of the corresponding $E(V)$ curve reported in Figure 1, i.e., $V = 580$ Å^3 for olivine, $V = 538$ Å^3 for β-spinel, and $V = 527$ Å^3 for spinel (all these volumes refer to the conventional unit cell of 56 atoms). For obvious reasons of electrostatics and chemical bonding, stable and metastable absorption sites for H$^+$ are located close to an O anion, with a bond length always close to that of the gas phase OH$^-$ (hydroxyl) ion (0.97 Å). Absorption sites, therefore, will be identified by the inequivalent O atom that binds H$^+$. Computations are started with H$^+$ close to the chosen O atom, and the geometry is optimized by a short MD annealing. Next, we characterized the energetics of the proton absorption by computing for different configurations the energy E_a defined by:

$$E_a = -[E(H^+ \mid Mg_2SiO_4) - E(Mg_2SiO_4) - E(H^+)] \text{ (9)}$$

The three energies on the right side are computed for simulation cells of the same volume and shape, and the charged systems are neutralized by homogeneous backgrounds of the same density. Of course, the E_a term defined above is not the quantity of direct interest in geophysical problems, because the protonated Mg$_2$SiO$_4$ is not in equilibrium with free protons. However, E_a directly gives the relative stability of different absorption configurations and can be used to compute thermodynamic

TABLE 3. Absorption energy

	E_a (eV)	d(OH) (Å)
Olivine		
O1	10.3	0.99
O2	11.5	1.05
O3	11.8	1.10
β-spinel		
O1	13.5	1.01
O2	12.5	1.09
O3	12.8	1.10
O4	13.0	1.06
Spinel		
O1	11.6	1.07

Absorption energy for H^+ close to each of the inequivalent O atoms in olivine, β-spinel, and spinel.

FIGURE 2. Low-energy absorption sites close to the O4 plane lying in a plane defined by the c and b direction. Units are given in Å. Large open circles = O4 atoms. Solid circles = Mg atoms. Circles with a plus sign = Si atoms below the O4 plane. Circles with a dot = Si atoms above the O4 plane. Small open circles = H^+ absorption sites close to the O4 plane.

quantities of more direct application by knowing the chemical potential of free protons with respect to the hydrated phases that are in equilibrium with Mg₂SiO₄ at mantle conditions.

Several stable or metastable positions correspond to each O atom. Our results for the lowest energy ones are given in Table 3. The most interesting case is, of course, β-spinel. A few years ago, Smyth (1987, 1994) and Downs (1989) suggested that the competition for the ground state is restricted to the O1 and O2 atoms: The first is favored by the longer distance from the Si ions and by the greater electronic charge, able to screen and bind the positive proton (Smyth 1987, 1994); the second was proposed by Downs on the basis of a careful analysis of charge-density distributions and electrostatic potential maps (Downs 1989).

A careful optimization of geometry and electronic structure confirms that indeed O1 is the most stable absorption site for H^+, with E_a = 13.5 eV and an equilibrium O-H distance of 1.01 Å. As mentioned above, O1 is at the center of the square basis of a pyramid formed by five Mg^{2+} cations. The proton is located outside the pyramid, on the prolongation of the line joining O1 to the apex Mg2, thus completing a (highly deformed) octahedral coordination shell for O1. In this position, the proton is relatively far from any other O atom (the closest one is O4 at 2.3 Å) and also relatively far from all the other cations.

The Mulliken population analysis shows that O1, which has an anomalous charge in the pure β-spinel structure (q = 1.43 e), acquires a "normal" charge in the hydrogenated case, i.e., it has a charge of q = 1.17 e, close to that of all the O atoms in olivine and spinel (q = 1.2 e) pure phases. The reduction of the ionic charge induces an outward relaxation of the O-Mg nearest-neighbor distances (by 0.25 Å) and a comparable relaxation for the O-Si nearest-neighbor distances. These results confirm the original intuition of Smyth (1987), attributing the special stability of $O1H^-$ to electronic structure effects, reflected in the underbonding of this O atom.

The special character of O1 is also evident in that it is the only relevant absorption site for which the proton is
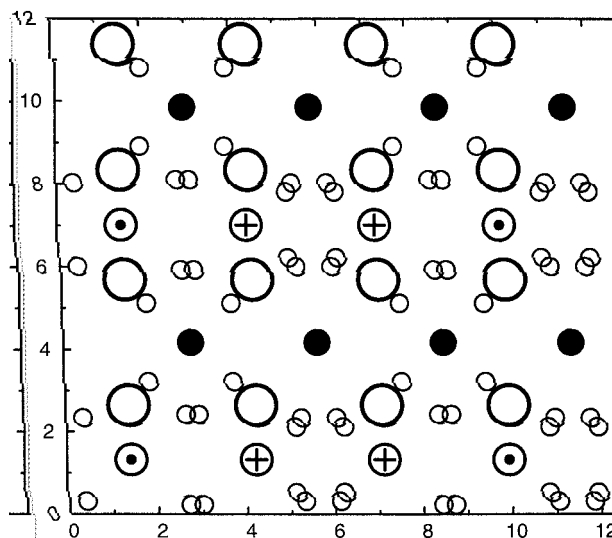
far from any other O atom. In all the other low-energy absorption sites the proton is shared between two O atoms, giving rise to a hydrogen bond. All these bonds are nearly linear and of the double-well type (Novak 1974), i.e., the proton is unequally shared by the two O atoms, and each site has a conjugate one, for which the role of the proximal and the distal O atom is interchanged. The two conjugate sites are equivalent when the hydrogen bond joins equivalent O atoms, inequivalent otherwise; the distance separating conjugate sites is short (0.5 Å at most), and the energy barrier among them appears to be small.

The most noticeable set of hydrogen-bonded absorption sites are those surrounding the O4 atoms, which provide the most stable position after O1. The O4 atoms are arranged on parallel planes separated by 4.1 Å, on which they form a nearly square lattice with a 2.7 × 2.85 Å unit cell, as depicted in Figure 2. The lowest energy among the absorption sites located close to this plane connects two O4 atoms belonging to the same Si₂O₇ unit and has an energy 0.5 eV higher than the O1 site. The sites connecting two O4 atoms belonging to different Si₂O₇ units have an energy 0.2 eV higher than the previous site. Slightly out of the O4 plane, and 0.05 eV higher in energy than the previous site (i.e., 0.75 eV higher than O1), is the site connecting an O4 to an O3 atom located in two different Si₂O₇ units. Its conjugate site, i.e., the one connecting the same pair of atoms but located closer to O3, has the same energy.

The O2 site, proposed in the past as an important absorption site because of a favorable electrostatic energy, is 1 eV higher in energy than the O1 site, and is, there-

fore, ~0.4 eV less stable than the O4 sites. Also absorption at O2 creates a hydrogen bond, but this is significantly distorted because of the interaction with nearby Mg^{2+} cations.

Computations for β-spinel at different volumes show that absorption energies decrease slightly with increasing pressure. This dependence is not strong enough to affect the relative stability of different absorption sites within each structure, and it is far less for different structures: By compressing β-spinel from 0 to 50 GPa (i.e., over a pressure range much wider than the stability range of Mg_2SiO_4 at the Earth mantle conditions), the absorption energy at O1 changes from 13.52 to 12.75 eV.

The importance of hydrogen bonding in stabilizing proton absorption is further highlighted by the comparison with the results for olivine and spinel. In olivine, the most stable absorption site is close to O3, and again creates a hydrogen bond. The bond, however, is somewhat distorted, and the absorption energy in this site is 1.7 eV less favorable than for β-spinel. Instead, at both the O1 and O2 sites, the H attached to O is separated from any other O atom by a plane of positive Mg^{2+} ions, preventing the formation of hydrogen bonds. The energy of both these sites is significantly higher. The most favorable absorption site in spinel corresponds to a local coordination similar to the one at O3 of olivine. Not surprisingly, the two absorption energies are similar, with H^+ at O1 in spinel being only 0.2 eV higher in energy than at O3 in olivine. The atomic coordinates for all the optimized hydrogenated structures are shown in Table 7.[1] The size dependence of our results was tested by repeating the computation in a larger system, with 16 Mg_2SiO_4 molecules and one proton. The energy differences among configurations and the absorption geometry do not change appreciably with size.

The large absorption energy difference between β-spinel and olivine implies a ratio for partitioning H^+ between the two phases that is much larger than the observed ratio 10:1 (Bell 1992; Young 1993; Inoue 1994). To reconcile the two results, we speculate that in the experiment the H distributions in the olivine and β-spinel samples were not fully equilibrated, and part of the H^+ in olivine might have been trapped at positions of local minima surrounded by large energy barriers.

H IN Mg₂SiO₄: MOLECULAR DYNAMICS SIMULATIONS

To check the stability of the optimized structures and to characterize the dynamics of the protonated β phase, we generated micro-canonical trajectories covering 1 ps after equilibrating the system at several temperatures from 400 to 1600 K. At the lowest temperatures the stretching of O1-H is remarkably harmonic, because the light mass of H decouples this mode from all the others (See Fig. 3). This allows a precise determination of its frequency, 3180 ± 30 cm⁻¹, in rather good agreement with 3322 cm⁻¹ recently reported on the basis of infrared and Raman spectra (McMillan 1991). Systematic devia-
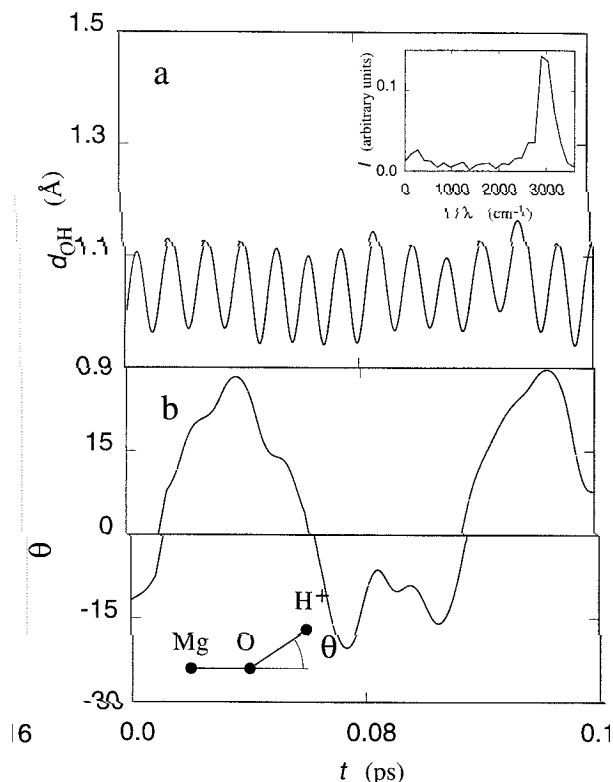

FIGURE 3. Stretching (*a*) and bending (*b*) motion of a proton absorbed at the O1 site (T = 800 K). The Fourier transform of the OH distance is shown in the inset.

tions in frequency because of the Car Parrinello dynamics of the Kohn-Sham states (discussed, for instance, in Onida 1994), were taken into account in the evaluation of ν and its error. The bending of the Mg-O-H bond is more difficult to characterize because of its longer period and its coupling with other modes (See Fig. 3). Our estimate for its frequency is ν = 350 ± 50 cm⁻¹, i.e., one order of magnitude lower than for stretching. As discussed below, this low bending frequency implies a large elongation of the lateral displacement for the proton and a high entropy contribution to the stability of the O1 site at high temperatures. At $T \geq 800$ K anharmonic effects become apparent in the H^+ motion, first in the bending and then in the stretching mode. The distribution of O atoms and the cations around a proton absorbed at O1 in β-spinel is reported in Figure 4 for T = 800 K. Up to T = 1400 K we do not observe any diffusion of the H^+ absorbed at O1. This result is not surprising: The next metastable position has an energy 0.6 eV higher and is separated both by a long distance and a high energy barrier, because each path to escape from O1 goes through narrow valleys delimited by cations. Most likely, the O1-H hydroxyl group is stable up to the melting temperature of Mg_2SiO_4.
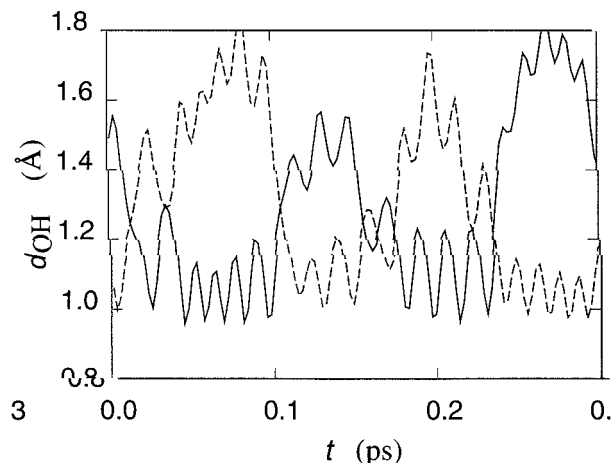
The dynamics of H^+ absorbed at the positions connecting two hydrogen-bonded O atoms is drastically different: The presence of two conjugate equilibrium sites at close distance, separated by a small barrier gives rise
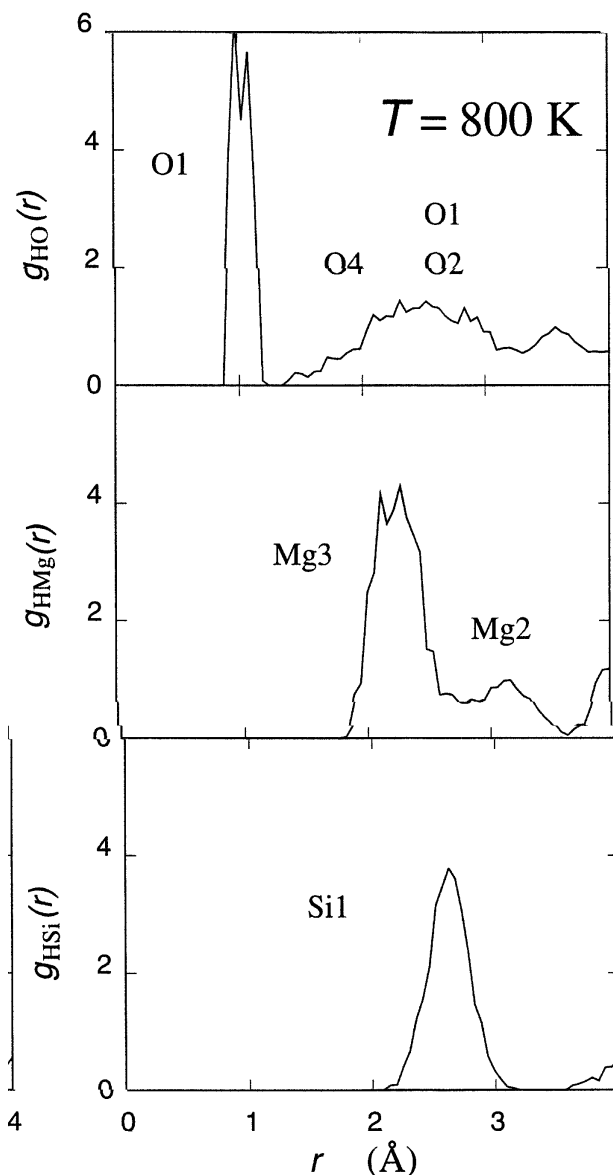
Figure 4. Radial distributions of O, Mg, and Si around a proton absorbed at the O1 position of β-spinel. The identities of the atoms contributing to each peak are identified according to the convention of Baur (1971).

Figure 5. Dynamics of a proton giving rise to a hydrogen bond between two O2 atoms in β-spinel (T = 850 K). The full and dashed lines give the distance of the proton to each of the two equivalent O atoms. The plateaus at d(OH) ≈ 1.1 Å and at d(OH) ≈ 1.5 Å correspond to the two equivalent minima along the hydrogen bond.

to a highly anharmonic motion, which is apparent already at low temperature. Even at 400 K, during the short time of the simulation, we observed several crossings of the proton between the double wells of the potential (e.g., Fig. 5). Nor did we observe any long range diffusion. The statistics over a period of 1 ps are apparently not sufficient to estimate the diffusion coefficient in the solid phase.

To estimate the role of entropy in determining the relative stability of different sites, we computed (by a simple MC integration) the volume visited in 1 ps by a proton absorbed at different sites. The sites favored most by entropy appear to be O4, because of the presence of long-range low-energy paths connecting them. Interestingly, the volume available for a proton at O1 is large, because of the large elongation associated with the soft-bending mode, implying that entropy will not counterbalance the special stability of this site even at high temperature. The volume available at disconnected hydrogen-bonded pairs (like those at the O2 sites) is significantly smaller. Despite the presence of a double minimum, the volume visited by a proton at O2 is one-half that available around O1 at the same temperature.

As a final computation for protonated β-spinel, we analyzed the interaction of one vacancy with the H$^+$ impurity. Computations were performed mainly with the system of 56 atoms. Additional computations with 112 atoms show that results do not depend much on the system size. As expected, over the entire range of distances covered in the 56 atoms cell, the interaction of the two impurities is repulsive; that of the protons with the vacancy is attractive. Because of efficient electronic screening at these defects, however, all these interactions do not appear to be very strong. The proton-vacancy interaction, in particular, is rather weak. Placing the two protons in the vacancy does not result in a stable or metastable configuration, although some electron charge is attracted by the two positive ions, forming at least part of the H$_2$ molecular bond. Also absorbing one H$^+$ at an O1 site and the other within the vacancy does not correspond to a stable or metastable configuration: A short MD annealing results in the migration of the proton from the vacancy to one of the closest O atoms. On the other hand, absorbing two protons at a single O site (giving a neutral H$_2$O water molecule), results in a metastable configuration only if the vacancy is very close (~2 Å) to the central O, otherwise the H$_2$O molecule breaks spontaneously

giving rise to two distinct OH^- groups. The stabilization, however, appears to be due more to the release of stress allowed by the empty Mg^{2+} position than to specific electrostatic or chemical interactions. For all the other positions of the protons absorbed to two different O sites, the total energy of the system does not change much (0.1 eV at most) by displacing the Mg^{2+} vacancy. The energy appears to increase monotonically with increasing distance between the protons and the vacancy.

REFERENCES CITED

Akaogi, M., Ross, N.L., McMillan, P., and Navrotsky, A. (1984) The Mg_2SiO_4 polymorphs (olivine, modified spinel and spinel)—Thermodynamic properties from oxide melt solution calorimetry, phase relations, and models of lattice vibrations. American Mineralogist, 69, 499–512.

Akaogi, M., Ito, E., and Navrotsky, A. (1989) Olivine-modified spinel transitions in the system Mg_2SiO_4-Fe_2SiO_4: Calorimetric measurements, thermochemical calculation, and geophysical application. Journal of Geophysical Research, 94, 15671–15685.

Akimoto, S. (1977) High-pressure research in Geophysics: Past, present and future. In M.H. Manghnani and S. Akimoto, Eds., High-pressure research in mineral physics, p. 1–13. American Geophysical Union, Washington, DC.

Baur, W.H. (1971) Geometric refinement of the crystal structure of β-Mg_2SiO_4. Nature Physical Sciences, 233, 135–137.

Bell, D.R. and Rossman, G. (1992) Water in earth's mantle: The role of nominally anhydrous minerals. Science, 255, 1391–1397.

Car, R. and Parrinello, M. (1985) Unified approach for molecular dynamics and density-functional theory. Physical Review Letters, 55, 2471–2474.

Ceperley, D.M. and Alder, B.J. (1980) Ground state of the electron gas by a stochastic method. Physical Review Letters. 45, 566–569.

Chopelas, A. (1991) Single crystal Raman spectra of forsterite, fayalite, and monticellite. American Mineralogist, 76, 1101–1109.

Downs, J.W. (1989) Possible sites for protonation in β-Mg_2SiO_4 from an experimentally derived electrostatic potential. American Mineralogist, 74, 1124–1129.

Finger, L.W., Hazen, R.M., and Yagi, T. (1979) Crystal structures and electron densities of nickel and iron silicate spinels at elevated temperature or pressure. American Mineralogist, 64, 1002–1009.

Galli, G. and Parrinello, M. (1991) Ab-initio molecular dynamics: Principles and practical implementation. In V. Pontikis and M. Meyer, Eds., Proceedings NATO ASI, computer simulations in materials science, p. 283–304. Kluwer, Dordrecht.

Hazen, R.M. (1976) Effect of temperature and pressure on the crystal structure of forsterite. American Mineralogist, 61, 1280–1293.

Hirsch, L.M. (1990) Enhancing mantle conductivity. Nature, 347, 232.

Hofmeister, A.M. (1987) Single-crystal absorption and reflection infrared spectroscopy of forsterite and fayalite. Physics and Chemistry of Minerals, 14, 499–513.

Hohenberg, P. and Kohn, W. (1964) Inhomogeneous electron gas. Physical Review B, 136, 864–871.

Horiuchi, H. and Sawamoto, H. (1981) β-Mg_2SiO_4: Single-crystal X-ray diffraction study. American Mineralogist, 66, 568–575.

Inoue, T. (1994) Effect of water on melting phase-relations and melt composition in the system Mg_2SiO_4-Mg_2SiO_3-H_2O up to 15GPa. Physics of the Earth and Planetary Interiors, 85, 237.

Jones, R.O. and Gunnarsson, O. (1989) The density functional formalism, its applications and prospects. Reviews of Modern Physics, 61, 689–746.

Karato, S. (1990) The role of hydrogen in the electrical conductivity of the upper mantle. Nature, 347, 272–273.

Kawada, E. (1977) The system Mg_2SiO_4-Fe_2SiO_4 at high pressures and temperatures and the earth's interior. Ph.D. Thesis. University of Tokyo.

Kleinman, L. and Bylander, D.M. (1982) Efficacious form for model pseudopotentials. Physical Review Letters, 48, 1425–1428.

Kohn, W. and Sham, L.J. (1965) Self-consistent equations including exchange and correlations effects. Physical Review A, 140, 1133–1138.

Lin, J.S., Payne, M.C., Heine, V., and McConnell, J.D.C. (1994) Ab-initio calculations on $(OH)^-$ defects in α-quartz. Physics and Chemistry of Minerals, 21, 150–155.

McConnell, J.D.C., Lin, S.J., and Heine, V. (1995) The solubility of Si^{4+} defects in α-quartz and their role in the formation of molecular water and related weakening on heating. Physics and Chemistry of Minerals, 22, 357–366.

McMillan, P.F., Akaogi, M., Sato, R.K., Poe, B., and Foley, J. (1991) Hydroxyl groups in β-Mg_2SiO_4. American Mineralogist, 76, 354–360.

Megaw, H.D. (1973) Crystal Structures. Saunders, Philadelphia.

Monkhorst, H.J. and Pack, J.D. (1976) Special points for Brillouin-zone integrations. Physical Review B, 13, 5188–5192.

Morishinta, H., Kato, T., Suto, M., Ohtani, E., Urakawa, S., Utsumi, W., Shimomura, T., and Kikegawa, T. (1994) The phase boundary between α- and β-Mg_2SiO_4 determined by in situ X-ray observation. Science, 265, 1202–1203.

Novak, A. (1974) Hydrogen bonding in solids. Correlation of spectroscopic and crystallographic data. Structure and Bonding. 18, 177–216.

Onida, G, Andreoni, W., Kohanoff, J., and Parrinello, M. (1994) Ab-initio molecular dynamics of C_{70}. Intramolecular vibrations and zero-point motion effects. Chemical Physics Letters, 219, 1–7.

Perdew, J.P. and Zunger, A. (1981) Self-interaction correction to density-functional approximations for many-electron systems. Physical Review B, 23, 5048–5079.

Pickett, W.E. (1989) Pseudopotential methods in condensed matter applications. Computer Physics Reports, 9, 115–197.

Ringwood, A.E. and Major, A. (1970) The system Mg_2SiO_4-Fe_2SiO_4 at high pressures and temperatures. Physics of the Earth and Planetary Interiors, 3, 89–108.

Ringwood, A.E. (1975) Composition and petrology of the earth's mantle. McGraw-Hill, New York.

Rubie, D.C. and Brearley, A.J. (1994) Phase transitions between β and γ $(Mg,Fe)_2SiO_4$ in the earth's mantle: Mechanisms and rheological implications. Science, 264, 1445–1448.

Smyth, J.R. (1987) β-Mg_2SiO_4—A potential host for water in the mantle? American Mineralogist, 72, 1051–1055.

——— (1994) A crystallographic model for hydrous wadsleyite (β-Mg_2SiO_4): An ocean in the earth's interior? American Mineralogist, 79, 1021–1024.

Stumpf, R., Gonze, X., and Scheffler, M. (1990) A list of separable, norm-conserving ab-initio pseudopotentials. Fritz-Haber-Institut Research Report, February 1990.

Sung, C.M. and Burns, R.G. (1987) Crystal structural features of the olivine-spinel transition. Physics and Chemistry of Minerals, 2, 177–197.

Szabo, A. and Ostlund, N.S. (1989) Modern Quantum Chemistry. McGraw-Hill,

Troullier, N. and Martins, J.L. (1991) Efficient pseudopotentials for plane-wave calculations. Physical Review B, 43, 1993–2006.

Wentzcovitch, R.M., Martins, J.L., and Price, G.D. (1993) Ab-initio molecular dynamics with variable cell shape: application to $MgSiO_3$. Physical Review Letters, 70, 3947–3950.

Wentzcovitch, R.M., Ross, N.L., and Price, G.D. (1995) Ab-initio study of $MgSiO_3$ and $CaSiO_3$ perovskites at lower-mantle pressures. Physics of the Earth and Planetary Interiors, 90, 101–112.

Wood, B.J. (1995) The effect of H_2O on the 410-kilometer seismic discontinuity. Science, 268, 1–76.

Wyckoff, R.W.G. (1968) Crystal structures. Interscience, New York.

Yin, M.T. and Cohen, M.L. (1982) Theory of static structural properties, crystal stability, and phase transformations: Application to Si and Ge. Physical Review B, 26, 5668–5687.

Young, T.E., Green II, H.W., Hofmeister, A.M., and Walker, D. (1993) Infrared spectroscopic investigation of hydroxyl in β-$(Mg,Fe)_2SiO_4$ and coexisting olivine: Implications for mantle evolution and dynamics. Physics and Chemistry of Minerals, 19, 409–422.

APPENDIX 1: PARAMETERS OF THE STATIC AND DYNAMICAL COMPUTATIONS

Static computations were performed using the code PWSCF written by S. Baroni (Scuola Internazionale Superiore di Studi Avanzati, Trieste, and Centre Européen de Calcul Atomique et Moléculaire, Lyon) and collaborators. The SGS pseudopotentials were used for Mg, Si, and O. Convergence was tested by performing systematic computations for E_c = 60, 80, and 100 Ry. A few additional computations were done for E_c = 110 Ry. These tests show that the kinetic energy cut off E_c = 100 Ry is sufficient to provide total energy differences among the different structures and different volumes to better than 0.6 mRy/atom.

The sampling of the BZ was performed using one special k point [(¼, ¼, ¼,) in reduced units (Monkhorst 1976)] for olivine and β-spinel. For spinel, having a smaller unit cell, we used two k points [(¼, ¼, ¼) and (¾, ¼, ¼)]. Convergence tests have shown that the error associated to the k point sampling is comparable to that due to kinetic energy cut off.

We used the electron gas data of Ceperley (1980), as interpolated by Perdew (1981), to evaluate the exchange and correlation energies.

To study the dynamics of H⁺ in Mg₂SiO₄ we performed an extensive set of ab-initio calculations in pure as well as H⁺-doped Mg₂SiO₄. To speed up these MD calculations we used a less demanding computation scheme. To this effect we generated soft pseudopotentials for O following the procedures of Troullier (1991) and used only the Γ point of the supercell. The calculations for pure Mg₂SiO₄ with SGS pseudopotentials, accurate sampling of the BZ, and the very high cut off presented here were used as the benchmark. With the soft pseudopotential and a cut off of 70 Ry, we were able to reproduce all the results obtained with the more accurate SGS pseudopotential. In orthorhombic cells of 56 and 112 atoms use of the Γ point also proved to be highly accurate.

The direct minimization of the energy functional and the ab-initio MD simulations were performed using the CPMD program (version 3.0) written by J. Hutter, Max-Planck-Institut für Festkörperforschung, Stuttgart.

Simulations were performed on an IBM RISC 590 workstation and required ~120 s of CPU for each MD step.

APPENDIX 2: THERMAL PROPERTIES BY AB-INITIO MOLECULAR DYNAMICS.

Molecular dynamics calculations for pure olivine, β-spinel, and spinel were performed as a preliminary exploration of the system dynamics and as a comparison with the simulations of protonated Mg₂SiO₄. All the parameters of these simulations were equal to those of the MD calculations described earlier. For each structure the volume was equal to the experimental equilibrium volume, and the temperature was set to ~700 K, representative of the conditions for a large portion of Mg₂SiO₄ in
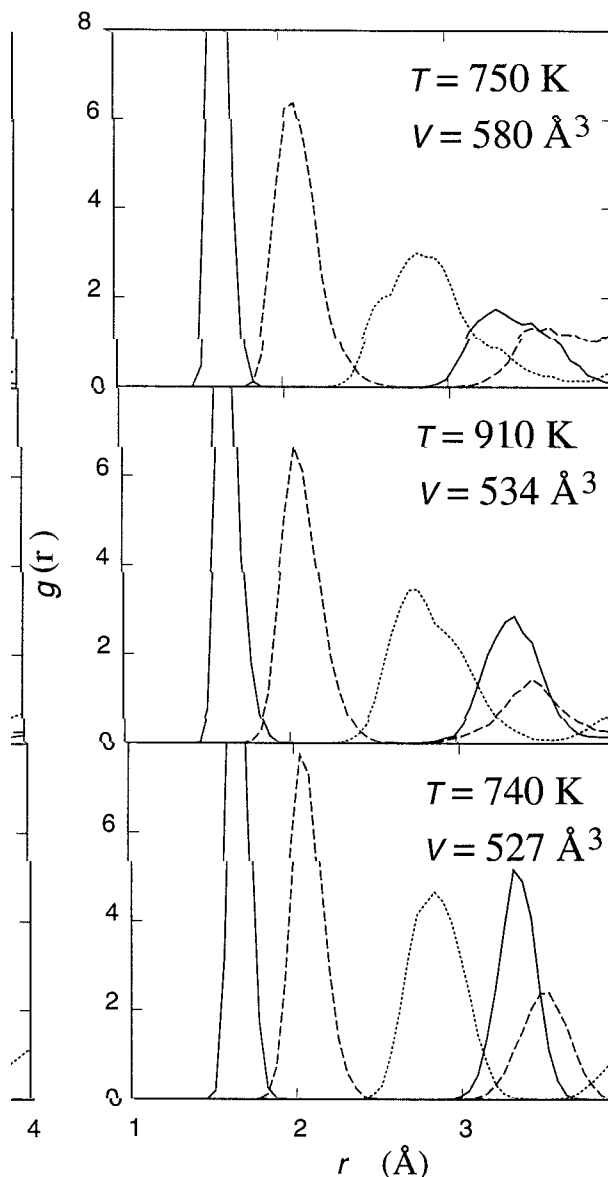
APPENDIX FIGURE 1. Radial distributions of Si (full line), Mg (dashed line), and O (dotted line) around a central O atom in the three polymorphs of Mg₂SiO₄ (top = olivine; middle = β spinal; bottom = spinel).

the upper mantle. For each structure, we equilibrated the system for ~3000 steps and accumulated statistics for 9000 steps, equal to 1 ps. The structures were characterized by the radial distribution functions, shown in Appendix Figure 1, and by the mean-square displacements of the different atoms, reported in Appendix Table 1. The main features of the radial distribution function are apparently very similar in the three phases, the only noticeable difference being in the shape of the first peak of the O-O correlation function. For all the structures, the atomic mean-square displacements reflect the strong localization of the Si atoms because of their high mass and strong

APPENDIX TABLE 1.   Atomic mean-square displacements ($Å^2$)

	Mg	Mg1	Mg2	Mg3	O	O1	O2	O3	O4	Si
Olivine		0.038	0.029			0.027	0.030	0.038		0.020
β-spinel		0.027	0.051	0.027		0.048	0.030	0.028	0.030	0.016
Spinel	0.022				0.020					0.010

Notes: The atomic mean-square displacements for olivine (at T = 750 K, V = 580 $Å^3$), β-spinel (at T = 910 K, V = 538 $Å^3$), and spinel (at T = 740 K, V = 527 $Å^3$) are estimated by a 1 ps MD simulation for a 56 atom sample. For all the data the statistical error is on the order of 0.002 $Å^2$.

bonding to four O atoms and the relatively soft restoring force for the Mg^{2+} cations. For each of the structures, the differences in the displacements for the inequivalent sites of each element are easily correlated with the local environment, with the details of the bonding discussed earlier. In β-spinel, for instance, the most delocalized O site is O1, apparently because of its underbonding due to the Mg^{2+} local coordination. Moreover, Mg2, which is the apex of the square pyramid that coordinates O1, is the most mobile of the Mg^{2+} cations and displays the largest displacement along the direction of the relatively soft O1-Mg2 bond. The full trajectories generated in our simulation are shown in Appendix Tables 2–6.[1]

[1] For a copy of Appendix Tables 2, 3, 4, 5, and 6, order Document AM-97-649 from the Business Office, Mineralogical Society of America, 1015 Eighteenth Street, Suite 601, Washington, DC 20036, U.S.A. Please remit $5.00 in advance. Deposit items may also be available on the American Mineralogist web site, refer to the inside back cover of a current issue for web address.